Volume 1 | Number 1 | Jan 2013 | Pages 1–100

RSC Advances

www.rsc.org/advances

RSC Advances

COMMUNICATION

Novel Eu-containing titania composites derived from a new Eu(III)-doped polyoxotitanate cage †

Yaokang Lv,[a,c,d] Zhiwei Cai,[a] Dongpeng Yan,[b]* Chang Su,[a] Weijun Li,[a] Wei Chen,[e] Zhuochao Ren,[f] Yongge Wei,[d] Ouyang Mi,[a,]* Cheng Zhang[a,]* and Dominic S. Wright[c,]*

The new Eu(III)-doped polyoxotitanate (POT) cage [$Ti_2O(OEt)_8(EtOH)EuCl]_2$ can be used as a single-source precursor to the formation of nanostructured Eu-containing titania composites and flexible fluorescent films, which exhibit significant red luminescence and are attractive fluorescent materials.

Lanthanide-containing materials have attracted considerable attention due to their common photocatalytic and luminescence properties.[1] As an abundant, technologically important, environmentally benign semiconductor, titania (TiO_2) is one of the ideal hosts for the accommodation of lanthanide ions.[2] In the past decades, considerable efforts have been devoted to the exploration of lanthanide-doped titania microspheres, nanoparticles and thin films.[3] These nanostructured titania materials of appropriate bandgap energies can act as effective light-harvesting antennae; absorbing light and then transferring energy to the lanthanide ion, from which then emit intense narrow-band luminescence.[4] However, there are still great challenges in preparing lanthanide ions doped homogeneously in titania, especially when high ion content is desired. Heterometallic polyoxotitanate (POT) cages are a developing class of inorganic compounds which can be regarded as nano- or sub-nano sized molecular relatives of metal-doped titania nanoparticles. These species not only serve as models for studying the ways in which dopant metal ions can be incorporated into metal-doped titania,[4] but also are useful as organically-soluble fragments to build stoichiometrically-

controllable advanced materials or hybrid assemblies.[5] In our previous study, bimetallic POT cages of the general type [$Ti_xO_y(OR)_z(Ce)$] were used to hydrolytically-deposit Ce(III)-doped titania with Ce(III) concentrations as high as 16 wt%, these materials exhibit exceptional broad-band absorption behaviour,[3b] but their fluorescence intensities were found to be relatively weak. On the other hand, it is known that Eu(III)-doped titania characteristically exhibit more intense emission and thus have possible applications in light-emitting devices.[6] Herein, we report a new Eu(III)-doped POT cage which can be used as a precursor to several titania composites, the micro-morphological, thermal and optical properties of which are investigated.

Solvothermal reaction of $Ti(OEt)_4$ with $EuCl_3$ in dry ethanol yielded large colourless crystals of cage [$Ti_2O(OEt)_8(EtOH)Eu^{III}Cl]_2$ (1) after slow evaporation of the solvent at room-temperature(ESI†). A single-crystal XRD study revealed that cage 1 has a $Eu_2Cl_2Ti_4O_{20}$ core, in which two Eu centres are associated by two bridging μ_4-O atoms (Fig. 1a). The eight-coordinated geometry of each of the symmetry-related Eu centres is completed by a terminal chloride ligand and by bonding to the O-atom of five ethoxy-ligands. The four Ti atoms of 1 have octahedral geometries and form two symmetry-related Ti_2O_9 subunits (Fig. 1b). The structure of 1 is similar to that found for the Ce derivative [$Ti_2O(OEt)_8(EtOH)Ce^{III}Cl]_2$.[3b]
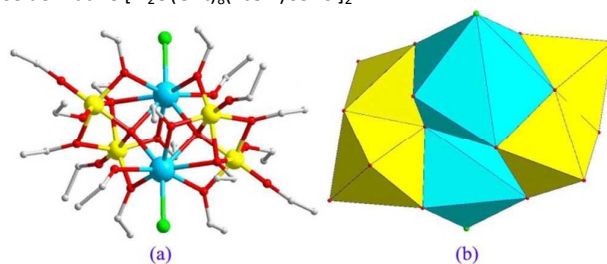

Fig. 1 (a) Solid-state structure of cage 1, H-atoms have been omitted for clarity (red = O, yellow = Ti, blue = Eu, green = Cl) and (b) polyhedral representation of the $Eu_2Cl_2Ti_4O_{20}$ core. Selected bond lengths and angles can be found in the ESI.

As shown in Fig. 2, cage 1 gives typical Eu(III) red emission under UV excitation. Similar to other reported POT cages,[4,5] crystals of cage 1 are readily soluble in a range of organic solvents such as toluene and dichloromethane (Fig. S1), but are easily hydrolyzed in ambient air (Fig. S2) and decompose when heating (Fig. S3). Based on these properties, we employed 1 as a single source material to a

[a.] College of Chemical Engineering and Materials Science, Zhejiang University of Technology, Hangzhou, 310014, P. R. China. Tel: 0086 571 88320253. E-mail: ouyang@zjut.edu.cn and czhang@zjut.edu.cn ;

[b.] College of Chemistry, Beijing Normal University Tel: 0086 10 64412131. E-mail: yandp@bnu.edu.cn;

[c.] Chemistry Department, Cambridge University, Lensfield Road, Cambridge CB2 1EW . Fax: 0044 1223 336362; Tel: 0044 1223 763122 E-mail: dsw1000@cam.ac.uk;

[d.] Department of Chemistry, Tsinghua University, Beijing 100084, P. R. China;

[e.] Department of Respiratory, Navy General Hospital, Beijing 100048, P. R. China;

[f.] Department of Respiratory, Zhejiang Provincial People's Hospital, Hangzhou 310014, P. R. China.

RSC Advances Accepted Manuscript

range of Eu-containing titania composites. Sonication of **1** in 50 v% aqueous ethanol gives a white powder **A** (Fig. 3a). The solid-state UV-visible reflectance spectrum of **A** shows a broad absorption band around 300–400 nm (Fig. S4), which is associated with the bandgap O(p)→Ti(d) transition in titania, some very weak bands also appear in the low-energy visible region (532, 466 and 426 nm), which correspond to the *f–f* ('free-ion') electronic transitions of the Eu^{III} ion. Powder-XRD analysis shows that **A** is amorphous (Fig. S5). The Scanning Electron Microscopy (SEM) (Figs. 3c) and Transmission Electron Microscopy (TEM) (Fig. 3d and **e**) images and the selected area electron diffraction (SAED) pattern (Fig. 3**e**) indicate that **A** is composed of ~5 nm size amorphous nanoparticles of TiO$_2$ agglomerated in micron-sized clusters. X-ray photoelectron spectroscopy (XPS) confirms that Eu is present as Eu(III) in **A**, Energy Dispersive X-ray Spectroscopy (EDS) reveals the mass percentage of Eu in composite **A** is about 28.4 %, with the observed Ti : Eu molar ratio being *ca.* 3 : 1 (ESI†). aA possible explanation for the difference between the ratio of Ti : Eu in the precursor **1** and in **A** is that TiO$_2$ is that the nanoparticles consist of a core of Eu(III)-doped TiO$_2$ coated with TiO$_2$ in a core-shell arrangement.[2b]
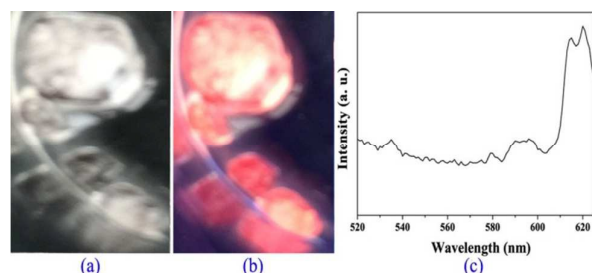

Fig. 2 (a) Optical image of crystals of cage **1**, (b) fluorescence image of the same sample of **1** under UV light irradiation of 254 nm, and (c) fluorescence spectrum of **1**, 1.0 × 10^{-4} mol L^{-1} in CH$_2$Cl$_2$ using 326 nm excitation.
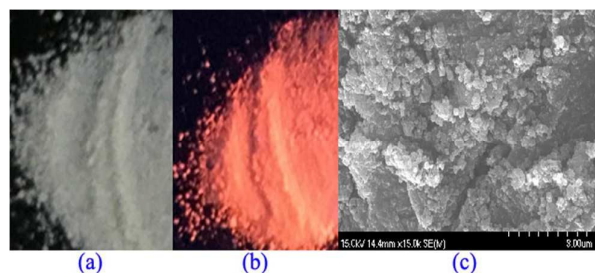

Fig. 3 (a) Optical image of powder of **A**, (b) fluorescence image of the same sample of **A** under UV light irradiation of 365 nm, (c) SEM image of **A**, (d) TEM image of **A** (e) HRTEM image of **A**, the inset shows the SAED pattern, and (f) fluorescence spectrum of **A** under 365 nm excitation.

As shown in Fig. 3b and Fig. 3f, **A** gives typical Eu(III) red emission, with the $^5D_0$-$^7F_0$, $^5D_0$-$^7F_1$, and $^5D_0$-$^7F_2$ peaks located at 581,

592 and 615 nm, respectively.[1d] To understand the excitation-state properties of **A** better, the fluorescence lifetime was also investigated. The decay profile has a double-exponential form with two lifetime values of τ_1 = 0.16 ms and τ_2 = 0.40 ms, which are close to the values seen in other Eu-based luminescent materials.[1e] The observed *ca.* 50 : 50 ratio of the two decay rates may be an indication that there are two types of chemical environment of Eu(III) in **A**.[1f,1g]

Calcination crystals of cage **1** at 500 °C in air gives off-white solid of **B** (Fig. 4a). Powder-XRD and Raman analyses indicate that **B** is a essentially a mixture of anatase TiO$_2$ and Eu(III)$_2$Ti$_2$O$_7$ (Fig. S5, S6). SEM analysis (Fig. 4b) reveals that **B** is composed of irregularly-shaped, *ca.* 0.5–5 μm microparticle agglomerates. The TEM image (Fig. 4c) indicates that **B** contains disordered nanoscale pores; the HRTEM image (Fig. 4d) and SAED pattern show that **B** also contains amorphous phase. XPS shows that Eu is also present as Eu(III). In contrast to the situation with **A**, EDS analysis reveals that there is a high degree of control of the average Ti : Eu ratio (ESI†), the observed molar ratio in **B** is around 2 : 1 (*cf.* 2 : 1 in the precursor cage **1**).
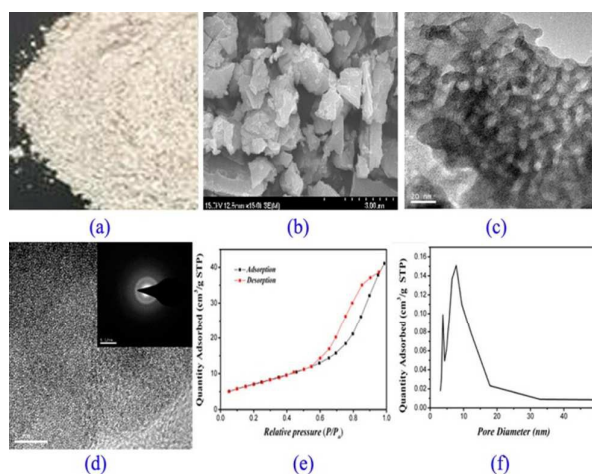

Fig. 4 (a) Optical image of **B**, (a) SEM image of **B**, (b) TEM image of **B**, (c) HRTEM image of **B**, the inset shows the SAED pattern, (e) nitrogen adsorption and desorption isotherms of **B**, and (f) pore size distributions in **B**.

As shown in Fig. 4e, the type IV nitrogen sorption isotherms of **B** exhibit a capillary condensation step at relative pressures of 0.6–0.9, suggesting the existence of hierarchical pore structure with different pore sizes from micro- to mesopores.[7] The Brunauer–Emmett–Teller surface area of **B** is around 26.34 m^{2}g^{-1} with the average pore size width of 9.65 nm; its pore size distribution, which is calculated from the desorption branch of the isotherm using the Barrett–Joyner–Halenda method, is in the range of *ca.* 3.0–32.8 nm (Fig. 4e). The nanoporous structure of **B** may result from the calcination processes involved in its formation, which results in the rapid oxidation of the organic residues present in the precursor **1**, leading to the rapid aggregation of the Eu-containing titania nanoparticles formed. We recently demonstrated a novel strategy to obtain nanoporous titania materials using the decomposition of POT cages,[8] the successful preparation of **B** indicates that homogeneous nanoporous metal-containing titania can also be

COMMUNICATION

fabricated *via* a similar strategy based on heterometallic POT cages.

Incorporation of cage **1** into poly-methylmethacrylate (PMMA) via solution blending (ESI†) gives film **P**. As shown in Fig. **5**, film **P** not only shows high transparency (Fig. 5a) and macroscopic flexibility (Fig. 5b) but also shows significant red luminescence under UV light irradiation (Fig. 5c). Compared with a blank PMMA film (**P$_0$**), film **P** displays improved thermal stability (Fig. S7), moreover, there are almost no particulates observed by SEM in the film (Fig. 5d), indicating uniform dispersion of cage **1** in the PMMA matrix. As shown in Fig. 5e, the emission spectrum of **P$_0$** exhibits a broad peak around 380nm, which is assigned to the PMMA matrix; however, four peaks are observed in the emission spectrum of **P**: the broad peak around 380 nm is much weaker than that for **P$_0$**, another three narrow peaks centered at 580, 592, and 615 nm (the strongest peak) are assigned to the $^5D_0 \rightarrow ^7F_0$, $^5D_0 \rightarrow ^7F_1$, and $^5D_0 \rightarrow ^7F_2$ transitions of Eu(III), the relative low red PL emission can be related to the fact that the Eu(III)-doped polyoxotitanate cage powders have been highly dispersed in the PMMA film matrix. Preliminary work indicates that the micro-morphological and fluorescence intensity of **P** can be adjusted by altering the conditions of incorporation (e.g. concentration of cage **1**, the drying procession, See ESI†).
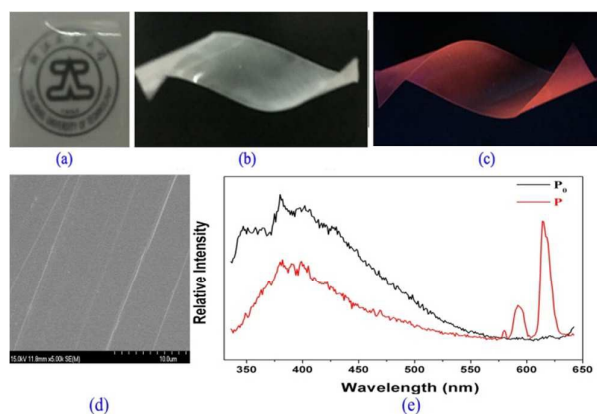

Fig. 5 (a) Optical image of **P** to demonstrate its visible-transmittance, (b) image of **P** to demonstrate its macroscopic flexibility, (c) photoluminescence image of **P** under 254 nm light irradiation, (d) SEM image of **P** (e) emission spectra under 326 nm excitation. (f) emission spectra under 326 nm excitation.

In summary, we have shown that the new organically- soluble Eu(III)-doped POT cage [Ti$_2$O(OEt)$_8$(EtOH)EuCl]$_2$ (**1**) can be used as a single-source precursor to fabricated different Eu-containing materials. Aqueous hydrolysis of **1** gives nanostructured Eu-containing titania composite **A**, calcination in air gives nanoporous composite **B** and incorporation of **1** into a PMMA matrix gives flexible fluorescent film **P**. The investigation of the optical behavior of **A** and **P** confirms that they exhibit significant red luminescence and both should be attractive fluorescent materials.

Notes and references

1   a) X. P. Cao, D. Li, W.H. Jing, W. H. Xing and Y. Q. Fan, *J. Mater. Chem.*, 2012, **30**, 15309-15315; b) N. Sabbatini, M. Guardigli and J. M. Lehn, *Chem Rev.*, 1993, **123**, 201-228; c) J. Silver, R. Withnall, *Chem. Rev.*, 2004, **104**, 2833–2856; d) A. F. Kirby and F. S. Richardson *J. Phys. Chem.*, 1983, **87**, 2557–2563; e) M. H. V. Werts, R. T. F. Jukes and J. W. Verhoeven, *Phys. Chem. Chem. Phys.*, 2002, **4**, 1542–1548; f) L. Wang, D. Yan, S. Qin, S. Li, J. Lu, D. G. Evans and X. Duan, *Dalton Trans.*, 2011, **40**, 11781-11787; g) R. Gao, M. Zhao, Y. Guan, X. Fang, X. Li, and D. Yan, *J. Mater. Chem. C*, 2014, **2**, 9579–9586.
2   a) L. Li, C. K. Tsung, Z. Yang, G. D. Stucky, L. D. Sun, J. F. Wang and C. H. Yan, *Adv. Mater.*, 2008, **20**, 903-908; b) Y. Lv, M. Yao, J. P. Holgado, T. Roth, A. Steiner, L. Gan, R. M. Lambert and D. S. Wright, *RSC Adv.*, 2013, **3**, 13659-13662; c) S. Obregón and G. Colón, *Chem. Commun.*, 2012, **48**, 7865-7867.
3   a) J. W. Stouwdam and F. C. J. M. van Veggel, *ChemPhysChem*, 2004, **5**, 743-746; b) S. J. Han, S. H. Choi, S. S. Kim, M. Cho, B. Jang, D. Y. Kim, J. Yoon and T. Hyeon, *Small*, 2005, **1**, 812-816; c) S. Forissier, H. Roussel, P. Chaudouet, A. Pereira, J. Deschanvres and B. Moine, *J. Therm. Spray Technol.*, 2012, **21**, 1263-1268.
4   a) Y. Lv, J. Cheng, A. Steiner, L. Gan and D. S. Wright, *Angew. Chem. Int. Ed.*, 2014, **53**, 1934-1938; b) Y. Lv, J. Cheng, P. D. Matthews, J. P. Holgado, J. Willkomm, M. Leskes, A. Steiner, D. Fenske, T. C. King, P. T. Wood, L. Gan, R. M. Lambert and D. S. Wright, *Dalton Trans.*, 2014, **43**, 8679-8689; c)Y. Lv, J. Willkomm, M. Leskes, A. Steiner, T. C. King, L. Gan, E. Reisner, P. T. Wood and D. S. Wright, *Chem-Eur J.*, 2012, **18**, 11867-11870; d) Y. Lv, J. Willkomm, A. Steiner, L. Gan, E. Reisner and D. S. Wright, *Chem. Sci.*, 2012, **3**, 2470-2473.
5   a) L. Rozes and C. Sanchez, *Chem. Soc. Rev.*, 2011, **40**, 1006–1030; b) F. Périneau, S. Pensec, C. Sassoye, F. Ribot, L. Lokeren, R. Willem, L. Bouteiller, C. Sanchez and L. Rozes, *J. Mater. Chem.*, 2011, **21**, 4470; c) Y. H. Lai, C. Y. Lin, Y. Lv, T. C. King, A. Steiner, N. M. Muresan, L. Gan, D. S. Wright and E. Reisner, *Chem. Commun.*, 2013, **49**, 4331-4333.
6   a) M. Chang, Y. Song, H. Zhang, Y. Sheng, K. Zheng, X. Zhou and   H. Zou, *RSC Adv.* 2015, **5**, 59314-59319; b) M. S. Attia, S. A. Elsaadany, K. A. Ahmed, M. M. El-Molla and M. S. A. Abdel-Mottaleb, *J. Fluoresc.*, 2015, **25**, 119-125.
7   a) S. Brunauer, L. S. Deming, W. E. Deming and E. Teller, *J. Am. Chem. Soc.* 1940, **62**, 1723–1732; b) Y. Lv, L. Gan, M. Liu, W. Xiong, Z. Xu, D. Zhu and D. S. Wright, *J. Power Sources*, 2012, **209**, 152-157.
8   J. Liu, Z. Cai, Y. Lv, Y. Zhang, C. Su, M. Ouyang, C. Zhang and D. S. Wright, *J. Mater. Chem. A,* 2015, **3**, 1837-1840.

RSC Advances Accepted Manuscript

Graphical Abstract

Synthesis and luminescence properties of novel Eu-containing titania composites based on a new Eu(III)-doped polyoxotitanate cage
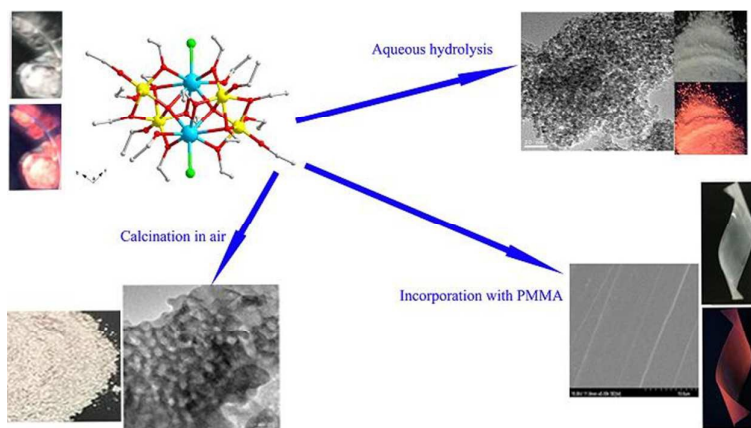
Y. Lv, Z. Cai, D. Yan, C. Su, W. Li, W. Chen, Z. Ren, Y. Wei, M. Ouyang, C. Zhang and D. S. Wright

The new cage $[Ti_2O(OEt)_8(EtOH)EuCl]_2$ (**1**) can be used as a single-source precursor to nano-structured Eu(III)-containing titania composites, nanoporous composites and flexible films; the latter two being attractive fluorescent materials.